Functionally Adaptive Structural Basis Sets of the Brain: A Dynamic Fusion Approach

Marlena Duda[1], Jiayu Chen[1], Aysenil Belger[2], Judith Ford[3,4], Daniel Mathalon[3,4], Adrian Preda[5], Jessica Turner[6], Theo Van Erp[7,8], Godfrey Pearlson[9], Vince D. Calhoun[1,10]

[1]Tri-Institutional Center for Translational Research in Neuroimaging and Data Science (TReNDS), Georgia State University, Georgia Institute of Technology, and Emory University, Atlanta, GA 30303, USA

[2]Department of Psychiatry, University of North Carolina, Chapel Hill, NC, USA

[3]Mental Health Service, San Francisco Veterans Affairs Healthcare System, San Francisco, CA, 94121, USA

[4]Department of Psychiatry and Weill Institute for Neurosciences, University of California San Francisco, San Francisco, CA, 94143, USA

[5]Department of Psychiatry and Human Behavior, University of California Irvine, Irvine, CA, 92697, USA

[6]Department of Psychiatry and Behavioral Health, Wexner Medical Center, The Ohio State University, Columbus, Ohio, 43210, United States

[7]Clinical Translational Neuroscience Laboratory, Department of Psychiatry and Human Behavior, University of California Irvine, Irvine, CA, 92697, USA

[8]Center for the Neurobiology of Learning and Memory, University of California Irvine, Irvine, CA, 92697, USA

[9]Departments of Psychiatry and Neuroscience, Yale University School of Medicine, New Haven, CT, USA

[10]Departments of Psychology and Neuroscience, Georgia State University, Atlanta, GA, 30302, United States

Abstract

The precise relationship between brain structure and dynamic neural function has long been an open area of research, and recently, a topic of much debate. Whether investigated through the lens of interregional white matter connectivity or cortical surface morphology, the common thread that links many studies in this subfield of research is the focus on identifying a singular structural basis set, upon which functional activation signals are reconstructed to define the linkage between structure and function. Such approaches are limited in two respects; first, these basis sets are defined solely upon structural data and ignore the influence of functional coupling entirely, and second, these approaches operate on the somewhat narrow assumption that a single structure-function coupling governs the activity of the whole brain at all times. The first limitation can be addressed with the use of multimodal data fusion, which identifies hidden linkages between structural and functional brain imaging data; however, many multimodal fusion approaches still necessitate functional data to be heavily summarized over the time dimension, resulting in temporally rigid structure-function linkages. Regarding the second limitation, given that functional brain activity and connectivity vary over multiple timescales, it is natural to consider this also might be true of structure-function couplings. Here, we introduce dynamic fusion, implemented as an ICA-based symmetric fusion approach, which enables flexible, time-resolved linkages between structure and function utilizing dynamic functional connectivity (dFNC) states. We show evidence that challenges current claims regarding structural basis sets and suggests that temporally evolving structural basis sets can better reflect dynamic functional manifolds and better capture diagnostically relevant structure-functional coupling than traditionally computed structural bases. Lastly, differential analysis of component stability across repeated scans from a control cohort reveals organization of static and dynamic structure/function coupling falls along unimodal/transmodal hierarchical lines.

Introduction

Over the last 50 years, advances in neuroimaging have produced a host of techniques capable of capturing detailed signatures of brain structure and function. Along with its incredible potential for revolutionizing diagnostics, the rise of neuroimaging has been instrumental in furthering investigation into one of the most fundamental questions in neuroscience: what is the relationship between brain structure and function? To this end, a class of approaches have been developed under the umbrella known as multimodal fusion, which aim to optimally integrate complementary data across various neuroimaging modalities. Multimodal fusion spans a wide range of techniques capable of revealing hidden linkages between imaging data types, and these techniques can be broadly divided into two categories: asymmetric

fusion approaches, wherein data from one modality are used to constrain or influence the analysis of another modality, and symmetric fusion approaches, wherein each imaging modality contributes equally to the combined analysis, fully leveraging the joint information across datasets (V. D. Calhoun & Sui, 2016; Sui et al., 2012).

In utilizing symmetric multimodal fusion to study the coupling between brain structure and function, there arises the common challenge of dealing with dimensional incongruence between "static" measures of brain structure and functional neuroimaging datatypes that include an additional temporal dimension. Historically, this has been addressed by heavily summarizing over the temporal dimension of the functional time series by computing measures such as static functional network connectivity (sFNC) (DeRamus et al., 2022) or amplitude of low-frequency fluctuation (ALFF) (Lottman et al., 2018), which does achieve dimensional compatibility of the data types for fusion, but also effectively removes the rich temporal information of the functional data. Some data driven approaches including group ICA + ICA (Qi et al., 2022) have been developed to handle mismatched data dimensionality, however these have not yet been expanded fully to leverage dynamics. With the surge in focus on functional dynamics over the last decade, the field has begun to recognize the significance of short-scale variation in connectivity (particularly during rest) and has pushed to preserve more temporal information in the analysis of fMRI data. A common output of dynamic functional network connectivity (dFNC) analysis is the identification of a small set of dFNC states or patterns that subjects move between during rest, often derived via k-means clustering (Allen et al., 2014). Several multimodal fusion studies have operated on the level of dFNC states by concatenating subject-level average connectomes across all states into a single FNC "mega-vector" in the fusion design (Abrol et al., 2017; Duda et al., 2022), thus enabling the inclusion of dynamic information into the multimodal fusion without increasing dimensionality of the functional inputs. Symmetric fusion approaches, such as multiset canonical correlation analysis with joint ICA (mCCA + jICA), were then applied to find hidden linkages between the concatenated dFNC and structural data, and functional patterns specific to each dFNC state were reconstructed post-hoc. While this approach enables some interpretation of state-specific linkages to structure, the resultant couplings are rather rigid as the concatenated dFNC components necessarily share a single loading parameter linking to a single structural component, imposing the (likely too strict) assumption that linkage to structure is identical across all dFNC states. Other joint approaches have investigated functionally informed structural basis sets (Plis et al., 2018) as well as individual linkages between specific intrinsic functional networks and structure (Khalilullah et al., 2023), but thus far there has been no framework for systematically identifying flexible structural basis sets based on linkages to time varying brain function.

On the flip side, widely used asymmetric fusion approaches are not bound by the same dimensionality constraints as symmetric fusions, at the cost of being less informative about the joint

relationship between modalities. One particular line of research that has recently emerged and can be classified under the umbrella of asymmetric fusion is the study of "structural brain modes". In short, structural graphs (which can be derived as white matter structural connectivity matrices via tractography analysis on diffusion MRI (Griffa et al., 2022) or maps of cortical surface geometry (Pang et al., 2023)) are subjected to eigenmode decomposition to obtain a singular structural basis set representing the so-called "structural harmonics" of the brain. These structural modes can be linked to brain function by projecting the fMRI signal at each timepoint as weights onto the discovered structural manifold. Such an approach does enable flexible linkage of structure to function over time through modification of the weights of the structural modes, however the rigid definition of a singular structural basis set without the influence of any linkage to function imposes a similar stringent assumption that all brain function can be sufficiently described by a static set of "functionally naive" structural modes.

It has long been known that functional brain activity and connectivity vary meaningfully over both long (across the lifespan) (Battaglia et al., 2020; Baum et al., 2020) and short (seconds to minutes) (V. Calhoun et al., 2010; V. D. Calhoun et al., 2014; Chang & Glover, 2010; Lurie et al., 2020; Preti et al., 2017) timescales, however the potential for similar temporal variation in structure-function couplings, especially at shorter timescales, has thus far been understudied. Most prior work has focused on either regional (Fukushima et al., 2018; Fukushima & Sporns, 2020) or temporal (Preti & Van De Ville, 2019; Vázquez-Rodríguez et al., 2019) fluctuations in structure-function coupling, but attempting to study simultaneous spatiotemporal fluctuation patterns of structure-function linkages is a relatively novel concept. One such work utilized multilinear regression to link regional measures of instantaneous functional connectivity to their structural connectivity profiles derived from diffusion MRI (dMRI) as an estimate of time- and region-resolved structure-function coupling (Liu et al., 2022). This study found that dynamic coupling patterns reflect cortical hierarchies, showing the strongest spatiotemporal fluctuations in the insula and frontal eye fields and the least in the unimodal and transmodal cortices. This atlas-based approach represents a critical initial dive into the space of temporally-evolving structure-function coupling at the level of data integration, and continued investigation into this space with advanced approaches like multimodal fusion promises to yield even deeper insights in this emerging domain of research by enabling joint estimation of data-driven structure-function linkages at the voxel level.

Here, we introduce an ICA-based symmetric fusion approach that allows for the identification of a temporally adaptive basis set that is inclusive of both structure and function, which we term "dynamic fusion". The following paper highlights three key results: 1) dynamic fusion-derived components of "static" structural MRI (sMRI) data capture clear task-related functional dynamics when applied in working memory task fMRI, 2) cross-fusion comparisons in resting state revealed a small set of relatively stable structural components, as well as a majority of "dynamic" structural components, and 3) dynamic

components exhibit stronger group differences in a schizophrenia (SZ) vs. control cohort. These results indicate that dynamic fusion enables flexible linkages between structure and time-evolving function which are related to changing cognitive demands, and suggest that the functionally influenced dynamic components may capture clinically relevant structure-function linkages that would be otherwise missed by standard approaches. In addition to fMRI/sMRI fusion experiments, we show similar results with dMRI as structural inputs to the dynamic fusion pipeline indicating measures of both white and gray matter show evidence for time-varying coupling to function.

Methods

Data & Preprocessing

We analyzed functional, structural, and diffusion MRI from the HCP 1200 (Van Essen et al., 2013) (N = 833 subjects, average age = 28.7 years) and FBIRN (Keator et al., 2016) (N = 310 subjects, N_{SZ} = 150 subjects [114 male, average age = 38.8 years], N_{CON} = 160 subjects [115 male, average age = 37.0 years]). datasets. Processing pipelines are detailed below:

fMRI: In both datasets, resting state fMRI data were preprocessed with a standard pipeline that included brain extraction, slice timing, and motion correction steps. Preprocessed data were then registered into structural MNI space, resampled to $3mm^3$ isotropic voxels, and spatially smoothed using a Gaussian kernel with a 6mm full-width-at-half-maximum (FWHM) on a per-subject basis. Spatially constrained ICA was applied using the GIFT toolbox (https://trendscenter.org/software/gift/) (Iraji et al., 2021) using the NeuroMark_fMRI_1.0 template (Du et al., 2020) to extract subject-level spatial maps and for each of the 53 intrinsic connectivity networks (ICNs) defined in the template, as well as their respective activation time courses. Dynamic FNC (dFNC) analysis of fMRI differed between the HCP and FBIRN datasets in an effort to explore consistency of our dynamic fusion approach relative to upstream pipeline designs.

In HCP, we utilized the REST1_LR and REST2_LR fMRI time series to perform repeated experiments within the same subject set and scan type. We computed dFNC in resting state fMRI from ICN time courses using a sliding window Pearson correlation (SWPC) approach outlined in (Damaraju et al., 2014), with the exception that the window size used in our analysis was 10 TR (~15s; TR = 0.72s). K-means clustering in resting state data revealed five dFNC states, and subject-average connectomes were computed for each state for dynamic fusion.

Of the 833 HCP subjects, 829 also had working memory (WM) task fMRI sessions. The WM tasks consists of four 27.5s task blocks with 15s rest blocks interleaved between each task. Applying

dynamic fusion in task-evoked fMRI enables the evaluation of the real-time adaptation of the neuroanatomical basis sets to known and structured functional changes across task boundaries. In the task data, we computed dFNC by sliding a 10 TR window starting from the last 15s of the first task block, across the first 15s rest block, and into the first 15s of the second task block, resulting in 12 windows each for pure Task 1, Rest, and Task 2, as well as 9 windows for each transition from Task 1→Rest and Rest→Task 2. For the WM task fMRI, we used surface data parcellated via (Glasser et al., 2016) using the hcputils package in python, and connectivity was computed via pairwise Pearson correlation between all 368 regions at each window.

In FBIRN, time and frequency resolved FNC patterns were computed from ICN time courses using the filter-bank connectivity (FBC) approach (Faghiri et al., 2021). Briefly, FBC utilizes a filter bank, i.e., an array of systems used to filter a time series into different frequency bands (typically non-overlapping and spanning the full frequency spectrum of the data), which enables estimation of FNC within a given frequency range. We designed our filter bank to contain 10 Chebyshev type-2 infinite impulse response filters that evenly cover the full frequency spectrum of the fMRI time series (0.00 – 0.25 Hz). K-means clustering identified six distinct states with unique connectivity signatures and spectral occupancy across frequency bands. In this work, we focus on three of the six states at the extremes of the frequency range: State 1 (low-frequency CON-dominant), State 2 (low-frequency SZ-dominant) and State 6 (high-frequency SZ-dominant) (Fig. 1). For more detail on the FBC approach and state clustering used here see (Duda et al., 2022).

sMRI: All structural data were preprocessed using statistical parametric mapping (SPM12) under the MATLAB 2019 environment. Structural images were segmented into gray matter, white matter, and CSF using the modulated normalization algorithm. The gray matter volume (GMV) map outputs were smoothed using a Gaussian kernel with FWHM = 10mm.

dMRI: The processing of dMRI data in HCP involves a series of steps using FSL (www.fmrib.ox.ac.uk/fsl), ANTs (Avants et al., 2009), and custom-built software. First, the datasets were collected with phase reversed blips, resulting in images with distortion in opposite directions. To address it, volumes containing b0 (b=5, with phase encoding in the left-right (LR) and right-left (RL) direction) were extracted from the entire set of 576 volumes for each dataset (comprising 3 LR runs with 95, 96 and 97 directions respectively, and 3 RL runs with corresponding directions). These b0 volumes were preselected by identifying the least-distorted pair, which was then used with topup (FSL 6.0)(Andersson et al., 2003) to estimate the susceptibility-induced off resonance field. The estimated fieldmap was used to unwarp the phased-encoded dMRI images. Next, the dMRI volumes underwent correction for eddy current distortions and head movement using eddy_gpu (FSL 6.0), which incorporated advanced motion-induced signal dropout detection and replacement (Andersson & Sotiropoulos, 2016). Subsequently,

Fractional Anisotropy (FA) maps were estimated from the diffusion tensor model using dtifit (FSL 6.0). The FA maps then underwent automated noise inspection, where any detected noise spots were padded with interpolation, and all FA values were adjusted to fall within the range of 0 to 1. Following this, the FA maps were registered to the Montreal Neurological Institute (MNI) standard space through nonlinear registration performed by ANTs. Any images exhibiting excessive motion, signal dropout, or excessive noise were excluded from subsequent analysis (Geenjaar et al., 2023; Wu et al., 2015).

Dynamic Fusion

We used multi-set canonical correlation analysis followed by joint independent component analysis (mCCA + jICA) to perform fusion of both static (GMV/FA maps) and temporally resolved (SWPC/FBC states) neuroimaging features. The combined mCCA + jICA model is designed to allow for the identification of both strongly and weakly correlated joint components that are also independent from one another. This is achieved by employing mCCA in the first step to generate flexible linkages between the modalities, and subsequently applying jICA to ensure independence between components. The ability to identify flexible (i.e., both strong and weaker) linkages between modalities is essential for the application to dynamic fusion, in which we are searching for nuanced differences in the joint information between structure and dFNC as a function of time, thus this requirement informed our design choice of employing mCCA + jICA as the symmetric fusion algorithm. The mCCA + jICA framework is defined under the assumption that a multimodal dataset, X_k, is a linear mixture of m sources (Sk) mixed by non-singular matrices (A_k), here, k = (1,2). The effective mCCA + jICA framework can be defined as $X_k = (D_k W^{-1})S_k$, where modality-specific mixing matrices are defined as $A_k = D_k W^{-1}$. Further details can be found in (Sui et al., 2011, 2013).

The key novelty in dynamic fusion is the concept of performing multiple data fusions which are linked together. In short, dynamic fusion generates functionally adaptive basis sets of brain structure by conducting multiple fusion experiments linking a static neuroanatomical measure (e.g., GMV map) to various distinct functional measures that represent temporally evolving functional patterns (Fig 1). We employ dynamic fusion at various levels of functional granularity in the experiments presented here. Using the HCP WM task data, we perform a window-level dynamic fusion wherein GMV maps are separately fused with each temporally evolving windowed FNC matrix (win = 10 TR = 7.2 seconds), focusing on the last 15 seconds of the first task block, across the full 15 seconds of the first rest block, and into the first 15 seconds of the second task block in order to assess the real-time stability and adaptability of the neuroanatomical basis to changing functional demands across task boundaries. Since subjects are not temporally aligned in resting state, window-level dynamic fusion would not be appropriate as the

underlying functional contexts/cognitive processes would not be fixed across subjects. Thus, to enforce some level of temporal and functional alignment in the resting state fMRI experiments, we perform state-level dynamic fusion wherein structural measures (either GMV or FA maps) are separately fused with subject-level state-average FNC matrices. All dynamic fusion experiments resulted in a set of structural (GMV or FA) components (model order = 10 or 15) optimized to each time-resolved FNC pattern (windowed FNC or state average) independently. Cross-fusion comparisons of these structural components across experiments revealed structural manifolds unique to each distinct functional basis (i.e., GMV/FA components related to frequency-specific functional connectivity dynamics), as well as some that were identified across multiple fusions, indicating a "static" structural component.

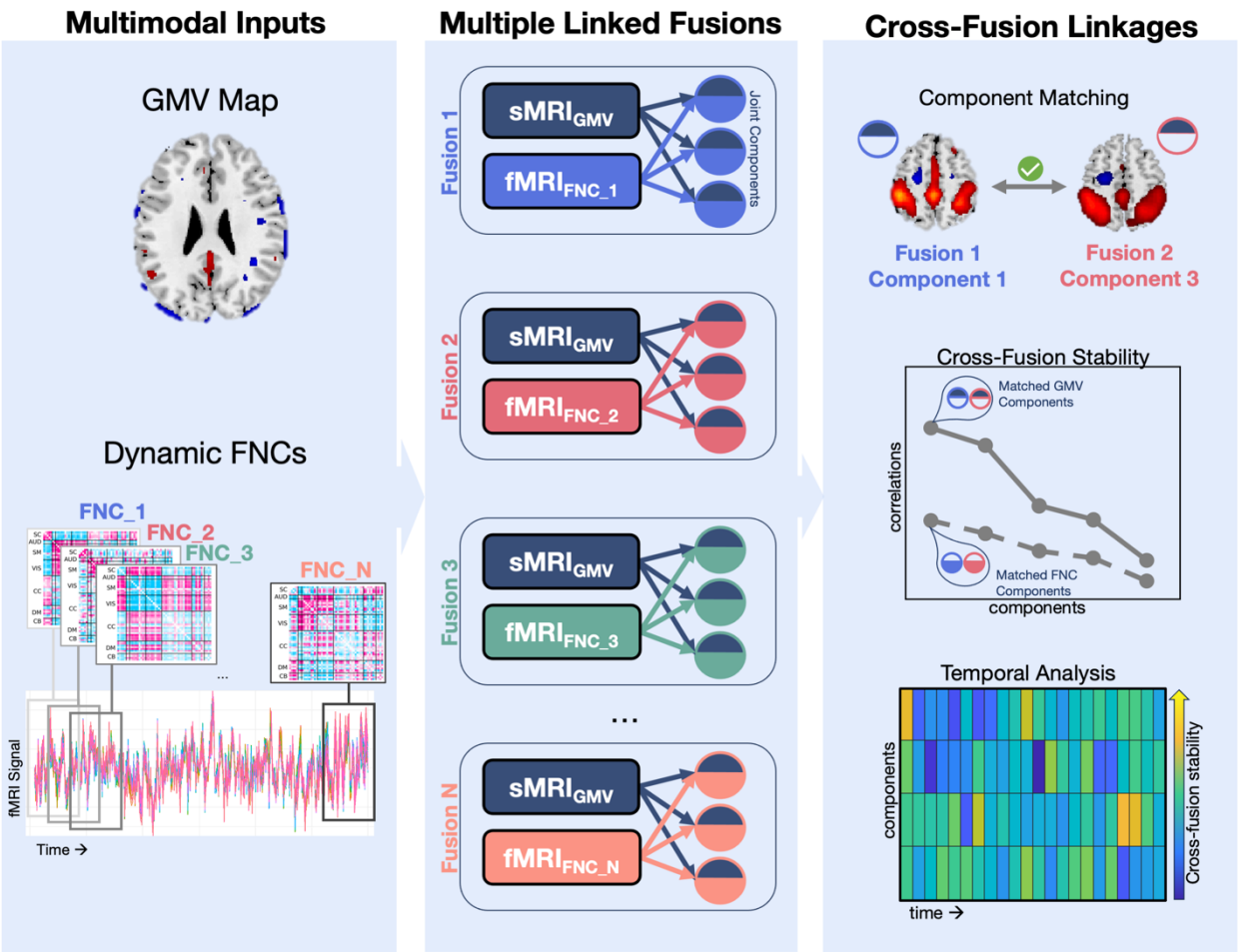

Fig 1. Schematic of dynamic fusion experimental design. Dynamic fusion links a single structural measure (i.e., GMV maps) to dynamic functional measures (i.e., windowed FNC matrices or subject average state connectomes) via multiple linked fusion experiments. Under the dynamic fusion framework, these can be performed as separate fusions to extract multiple functionally influenced structural basis sets.

Post-hoc cross-fusion analysis is performed to assess the stability of both the structural and functional components derived across the linked fusions, as well as their temporal evolution over time.

Results

Structural Components Reflect Working Memory Task Dynamics

We performed sliding window dynamic fusion in the HCP WM task data to determine whether task boundaries encoded in functional data could be detected strictly from the stability of the structural GMV component maps derived from fusions with respect to the changing functional manifold over time. Results are presented in Fig 2. We used a greedy matching technique to match component maps from fusions at consecutive windows and plotted the cross-fusion correspondence of consecutive component matches as measured by Pearson correlation. We observed the emergence of structural stability in different components in clear relation to known task boundaries. Component 1 shows high stability during Task 1, which drops off once Rest timepoints are included in the window. Component 5 exhibits the emergence of high stability at the onset of the Rest block, which drops through the Rest/Task 2 merged windows and disappears fully at the start of Task 2. Further, Component 9 shows high stability aligned with the Task2 block that was notably absent during Task 1. There is some evidence for block-related stability in Components 2 and 3 during Rest and Task 2, respectively, but to a lesser degree than components 5 and 9. By design, the structural input is identical at each windowed fusion, thus any variation in the resultant GMV components can be attributed to the changing functional manifold at each window and the evolution in the hidden structure-function linkages identified via mCCA + jICA. These results serve as a proof of concept that task-related functional dynamics can be encoded in structural GMV components under the dynamic fusion framework.

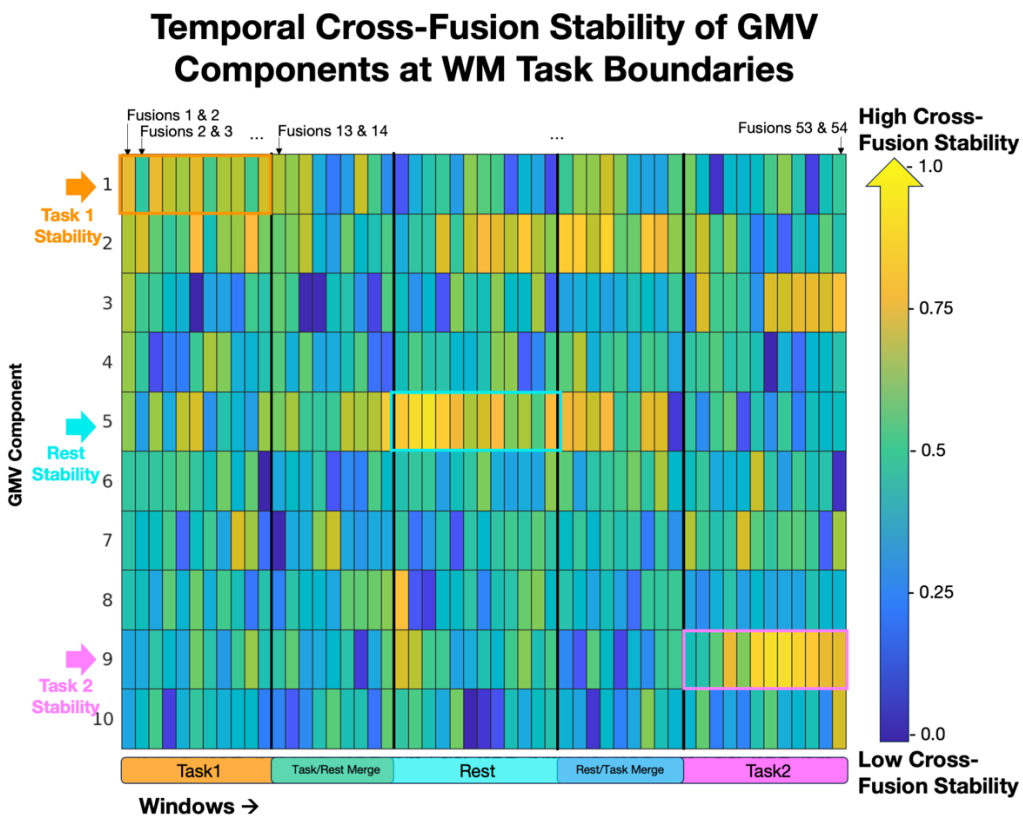

Fig 2. Temporally evolving cross-fusion correspondence between matched GMV components captures clear task-related functional dynamics in certain components. Each column represents a comparison between two separate data fusions using dFNC data computed from consecutive windows in the working memory (WM) task.

Resting State Dynamic Fusion Uncovers Both Static and Functionally Influenced Structural Components

In both the HCP and the FBIRN datasets, we performed state-level dynamic fusion of GMV maps with different metrics of dFNC for each dataset (FNC via SWPC in HCP and FBC in FBIRN). Findings across the two datasets were consistent. Fig. 3 illustrates the cross-fusion stability of GMV (solid lines) and FBC/FNC (dashed lines) component maps for both HCP (left) and FBIRN (right) experiments. We observed low correspondence overall for the functional components (dashed lines), which was expected as each of the functional inputs (dFNC states) have unique connectivity signatures, and, in the case of the FBIRN experiments, are even found in distinct frequency bands. Though the GMV components exhibited higher stability overall, we observed varying degrees of correspondence between best-matched GMV components across independent fusion experiments, even though the structural inputs were identical across each fusion. Specifically, we found fairly high cross-fusion correspondence ($|r| > 0.55$) in only the

first few components followed by a fairly steep drop-off of component correspondence, indicating little overlap between a majority of the resultant components. These consistent results across the two datasets suggest most of the structural components identified via mCCA + jICA are functionally influenced (i.e., "dynamic"), while a small subset are not functionally influenced (i.e., "static"). This result further demonstrates the ability of symmetric fusion approaches like mCCA + jICA to identify truly joint linkages in the data, as the changes in the functional inputs resulted in considerably different structural outputs, despite accounting for a much smaller portion of the entire dimensionality of the original input data. Moreover, our findings underscore the importance of enabling flexible linkages between structure and changing function, as arbitrarily imposing a limited structural basis would obfuscate the differential structure-function linkages that we have identified via dynamic fusion.

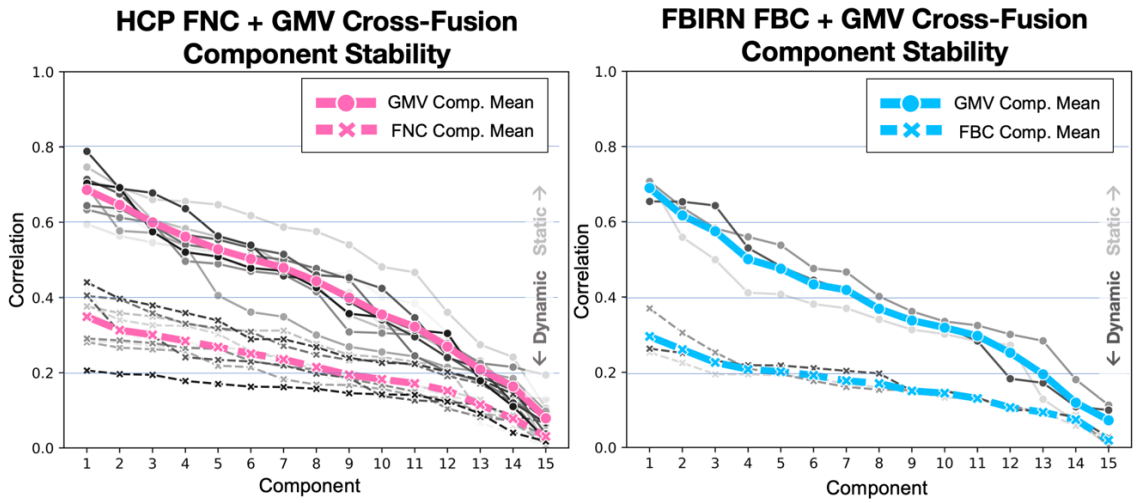

Fig. 3. State-level dynamic fusion in HCP and FBIRN datasets reveals a small set of static structural components and a larger set of functionally influenced components.

Significant Schizophrenia/Control Group Differences were identified in both Static and Dynamic Components

For each of the 45 components derived across the three linked FBIRN state-level dynamic fusion experiments (model order = 15), we computed group differences between the GMV component loading parameters (FDR corrected for multiple comparisons) and defined each component as "static" or "dynamic" (i.e., functionally uninfluenced or functionally influenced) based on the average cross-fusion correlation > or < 0.5 across all pairs of cross-fusion experiments, respectively (Fig. 4). We found 6/10

static components exhibited significant group loading differences, as well as (15/35) dynamic components. In fact, the significance levels of many of the dynamic components is directly on par with those of the static components. These results further highlight the utility of functionally influenced dynamic structural components in capturing clinically and diagnostically relevant features of structure-function coupling that are otherwise missed in the static components. In Figures 5 and 6, we visualize the joint sources and highlight group effects for some of the most significant components from both the dynamic and static sets.

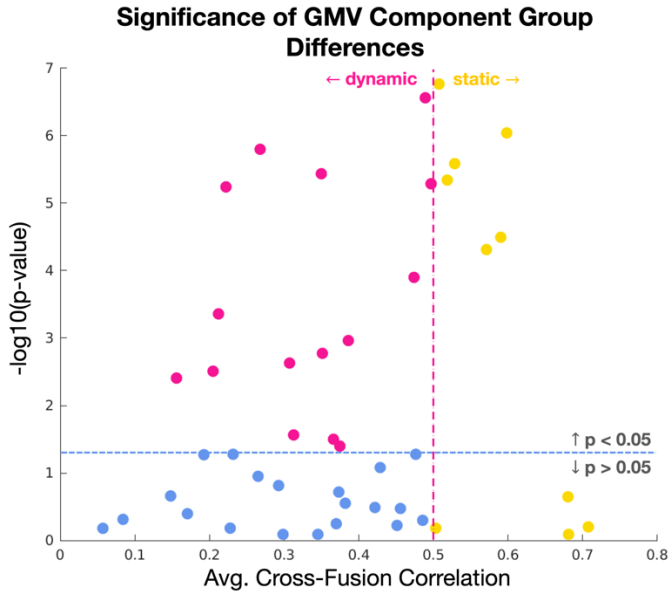

Fig. 4. Significance of group differences of GMV component loading parameters vs. average cross-fusion correlation (i.e. component map stability across state-level dynamic fusion experiments).

Joint sources for a pair of static components exhibiting significant group differences in loading parameters are shown in Fig 5. Static Joint Source 1 was derived from fusion with functional data from a CON-dominant low-frequency state (State 1 in (Duda et al., 2022)), and exhibited an average cross-fusion correlation of 0.598 as well as group differences in GMV component loading parameters at a significance level p = 9.14e-07. Static Joint Source 2 was derived from fusion with functional data from an SZ-dominant low-frequency state (State 6 in (Duda et al., 2022)), and exhibited an average cross-fusion correlation of 0.530 as well as group differences in GMV component loading parameters at a significance level p = 2.61e-06. Though both derived from fusions with vastly different functional contexts, as underscored by the lack of overlap in most edges in the functional components for each joint source, the structural component maps are highly similar across the fusions (r = 0.638), with peaks in anterior cingulate and orbitofrontal regions. These paired sources illustrate structural components that are not strongly influenced by their link to function, which can be understood as “static” or “global” structural

components. This is also reflected in the joint histograms depicting loading parameter group differences – across both joint sources the SZ and CON groups are more readily separable across the structural loading axis and more overlapped across the functional loadings axis, suggesting an overall weaker influence of the functional inputs compared to the structural inputs to the entire joint source.

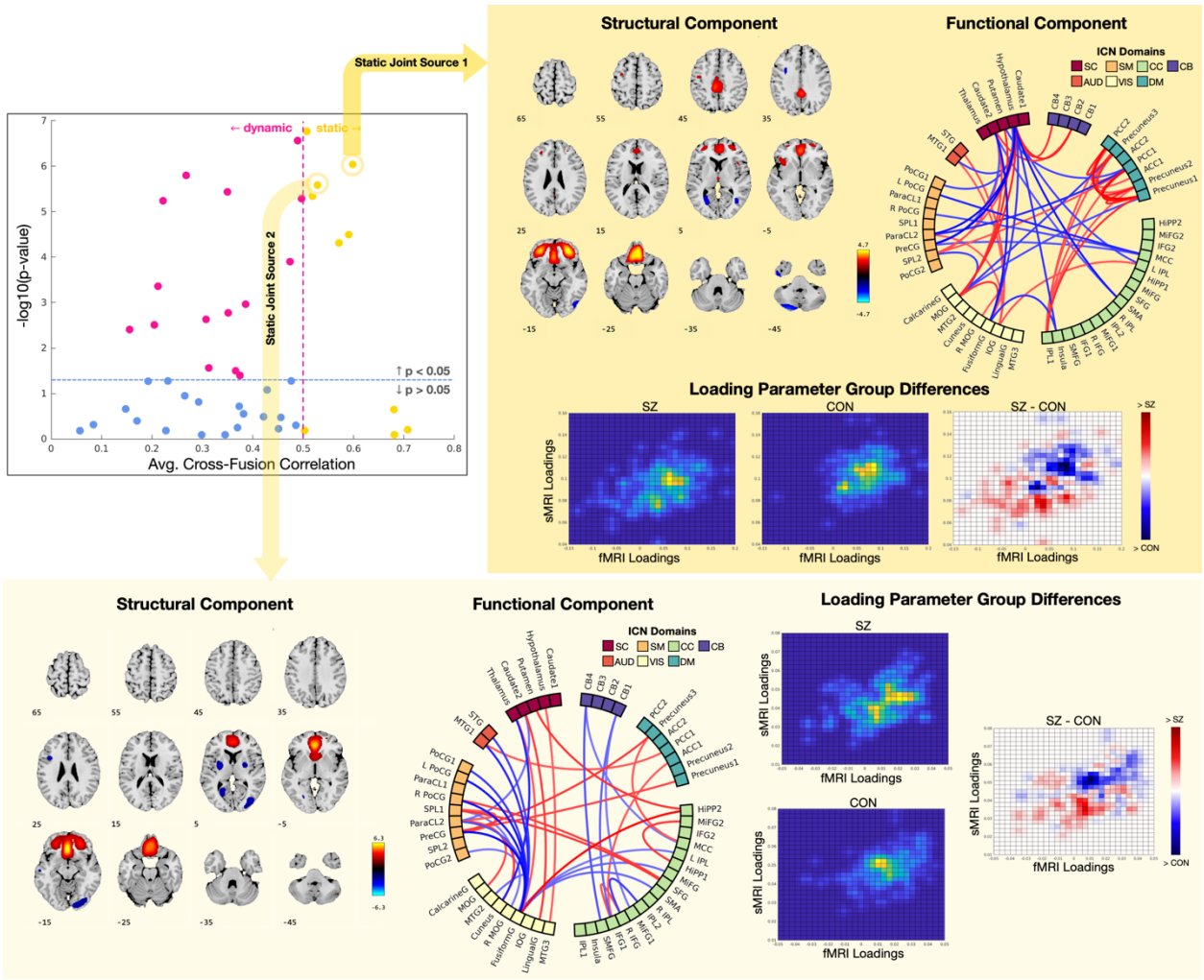

Fig. 5. Joint sources of paired static components with significant group differences in loading parameters. Static Joint Source 1 was derived from dynamic fusion to a CON-dominant low-frequency state (State 1), while Static Joint Source 2 was derived from dynamic fusion to an SZ-dominant high-frequency state (State 6). Structural component maps are highly similar, both exhibiting peaks in anterior cingulate and orbitofrontal regions, while linked functional components show little overlap. See (Duda et al., 2022) for more details on FBC states. Abbreviations: subcortical (SC), auditory (AUD), sensorimotor (SM), visual (VIS), cognitive control (CC), default mode (DM), cerebellum (CB), schizophrenia (SZ), control (CON).

We highlight two dynamic joint sources in Fig. 6. Both Dynamic Joint Sources 1 and 2 were derived from dynamic fusion to an SZ-dominant low-frequency state (State 2 in (Duda et al., 2022)). Dynamic Joint Source 1 exhibits peaks across the cingulate cortex, has an average cross-fusion correlation of 0.489 and group differences in structural component loading params at the significance level $p = 2.76e-07$. Dynamic Joint Source 2 exhibits peaks in default mode regions, has a much lower average cross-fusion correlation of 0.222, indicating it did not readily match components derived from the other state fusion experiments, yet still exhibited strong group differences in structural component loading params at the significance level $p = 5.77e-06$. As expected, the functional components for each dynamic joint source and unique, with Dynamic Joint Source 1 exhibiting CB-DM/CB-VIS correlations and CC-CB/CC-DM anticorrelations and Dynamic Joint Source 2 exhibiting positive CB-AUD/CB-VIS (marked by a hub in cerebellum 4 region) and negative CB-SC/CC-SM edges (marked by a hub in the insula). Further examination of the dual histograms of loading parameter group differences, we observe tighter concentration of SZ and CON subjects within both the structural and functional loading parameter spaces than was observed for the static sources, as well as more distinct separability of the groups in both the structural and functional parameter axes, suggesting a stronger contribution of both inputs into the joint solution.

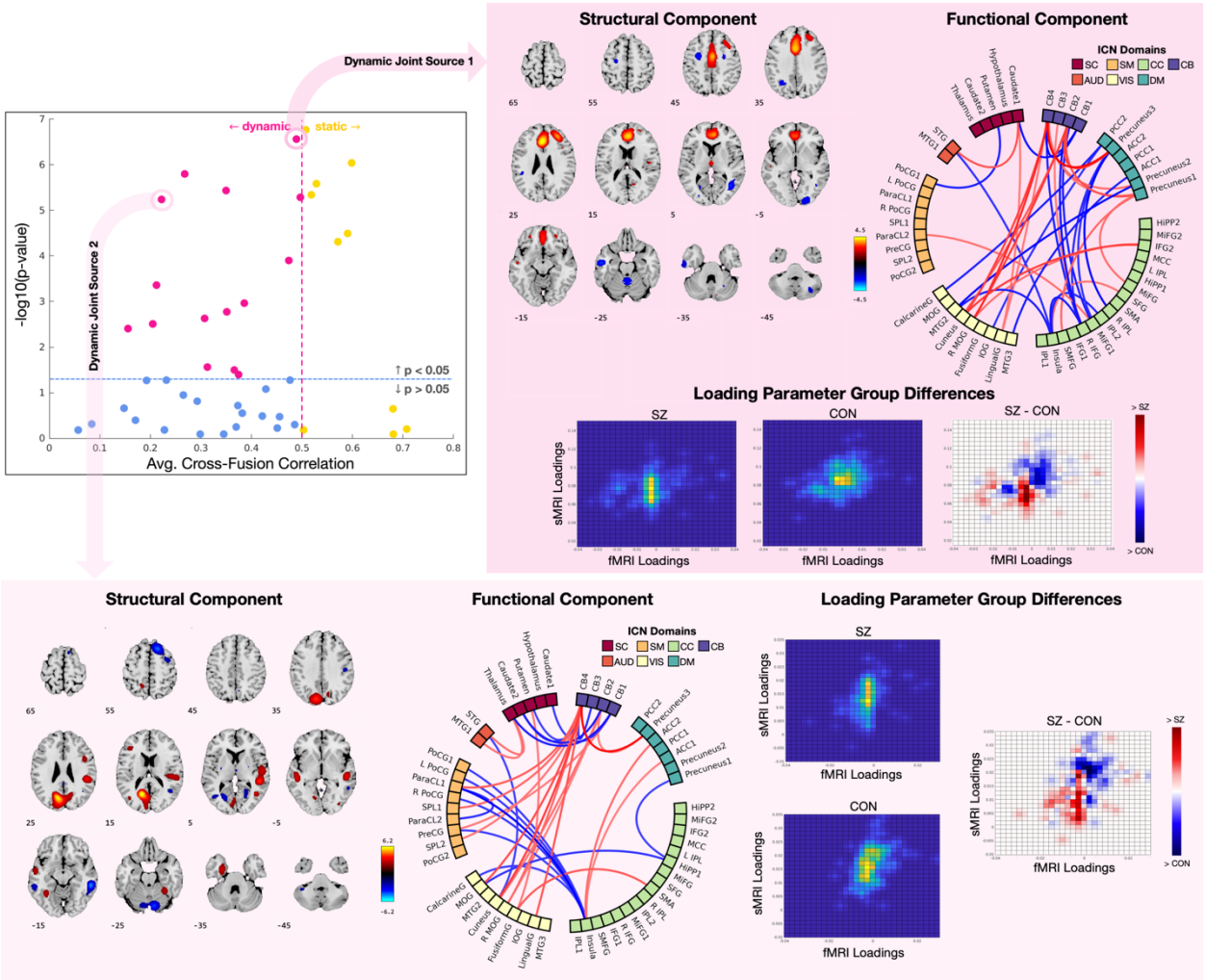

Fig. 6. Joint sources of two exemplar dynamic components with significant group differences in loading parameters. Both Dynamic Joint Sources 1 and 2 were derived from dynamic fusion to an SZ-dominant low-frequency state (State 2). The structural map for Dynamic Joint Source 1 shows peaks in the cingulate cortex, while the structural map for Dynamic Joint Source 2 shows peaks in default mode regions. Joint loading histograms show tight concentration of both SZ and CON subjects, and strong separations on both the structural and functional component axes, indicating strong contributions of both the structural and functional data to the joint sources. See (Duda et al., 2022) for more details on FBC states. Abbreviations: subcortical (SC), auditory (AUD), sensorimotor (SM), visual (VIS), cognitive control (CC), default mode (DM), cerebellum (CB), schizophrenia (SZ), control (CON).

Organization of Static/Dynamic Structure/Function Coupling in Healthy Brains Aligns to Unimodal/Transmodal Hierarchical Segregation of Cortex

After establishing both the cognitive relevance (Fig 2) and clinical utility (Figs 4-6) of joint sources derived via dynamic fusion, we aimed to conduct an exploratory analysis in a healthy control cohort (HCP) in attempts to reveal any underlying organization of the brain into hubs of largely static or largely dynamic structure-function linkage. Thus, we applied our dynamic fusion pipeline in both HCP REST1_LR and REST2_LR fMRI time series (henceforth termed Rest_1 and Rest_2), collected with the same scan parameters on the same subjects on both their initial and return study visits (Van Essen et al., 2013). In both experiments, 5 dFNC states were derived via k-means and model order = 15 were used for fusion, resulting in 75 joint sources each for both Rest_1 and Rest_2. As was done in the FBIRN analysis, greedy cross-fusion matching and correlation of structural component maps was performed separately in both experiments, and components were ranked and labeled as "dynamic" or "static" according to their stability score (i.e., average cross-fusion correlations) < or > 0.5, respectively. After filtering of spurious components, we selected the top 10 most static (i.e., highest stability scores) and top 10 most dynamic (i.e., lowest stability scores) components. For each set of static/dynamic components, component maps are aggregated as follows: first, component maps are thresholded for significance ($|z| >= 2$), then $|z|$ maps are normalized to [0, 1], weighted by stability score (or 1-stability score in the case of dynamic components), and aggregated by taking the max value at each voxel. For both experiments, we subtract the dynamic map from the static map to obtain composite differential stability maps across the whole brain, and finally average the Rest_1 and Rest_2 maps to obtain a global view of brain organization into statically/dynamically linked regions (Fig 7).

From the structural differential stability map, we can observe the organization of the brain into clear hubs of static and dynamic structure/function linkage, as well as mixed regions that exhibit both properties. Static hubs are comprised mostly of regions in the anterior cingulate and visual regions, whereas dynamic hubs are found in the insula, default mode regions and subcortical structures. These patterns are also reflected in the differential functional component map – the insula, inferior parietal lobule, posterior cingulate, precuneus and subcortical structures including putamen and caudate are all marked by stronger edges in dynamic components, whereas visual, sensorimotor and anterior cingulate regions all serve as hubs for edges in predominantly static joint sources. We note that our results align well to the widely-studied unimodal-transmodal principal functional gradient (Margulies et al., 2016), where we find static hubs align to the extremes of the unimodal (i.e., visual cortex) – transmodal (i.e., association cortex/anterior cingulate regions) cortical structures, whereas dynamic hubs are comprised of intermediary regions along this gradient (i.e., insular cortex). This organization of time-varying structure-function coupling throughout the brain quite closely mirrors recent work published in (Liu et al., 2022).

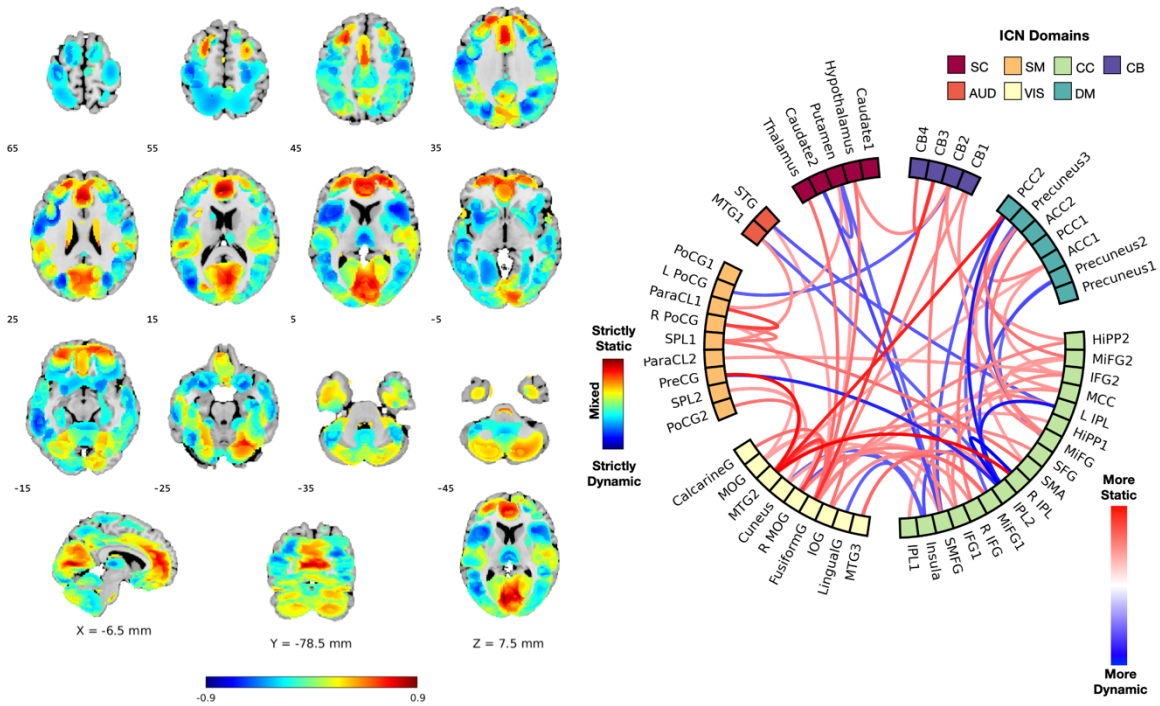

Fig. 7. Average of Rest_1 and Rest_2 differential stability maps in both structural and functional components. Structural maps reveal organization of the brain into regions hallmarked by static (anterior cingulate, visual regions) and dynamic (default mode, subcortical regions, insula) structure/function linkages. This segregation aligns well to unimodal/transmodal hierarchical lines.

White Matter Components Show Strong Links to Temporally Evolving FNC

Of the total 833 HCP subjects, 737 had processed FA maps available, thus we replicated the state-level HCP dynamic fusion experiments in this subset of subjects using white matter FA maps as the structural inputs with model order = 10. Results comparing the GMV and FA dynamic fusion experiments with the same model order are shown in Fig 7. While the overarching relationship between structure and function holds in the FA data (higher stability in structural components than functional components), there are a few key differences to highlight. First, the FA experiment shows evidence for just one highly static (mean cross-fusion correlation = 0.75), with a steep drop-off to the rest as dynamic components, as opposed to a gradual decrease in cross-fusion stability and two or three "static" component maps. Second, the overall cross-fusion stability of the components is lower in the FA experiments compared to GMV. This result may suggest a stronger linkage to the changing functional manifolds in each distinct dFNC state fusion, thus leading to lowered cross-fusion stability. To assess this hypothesis, we compared the correlations between the structural and functional loading parameters for all components in the GMV and FA

experiments and found that the correlations were indeed higher in the FNC + FA components ($p = 0.0043$, $t = -2.927$). These results may suggest that white matter FA components can be more susceptible to influence of changing functional inputs than GMV maps in symmetric data fusion approaches like mCCA + jICA.

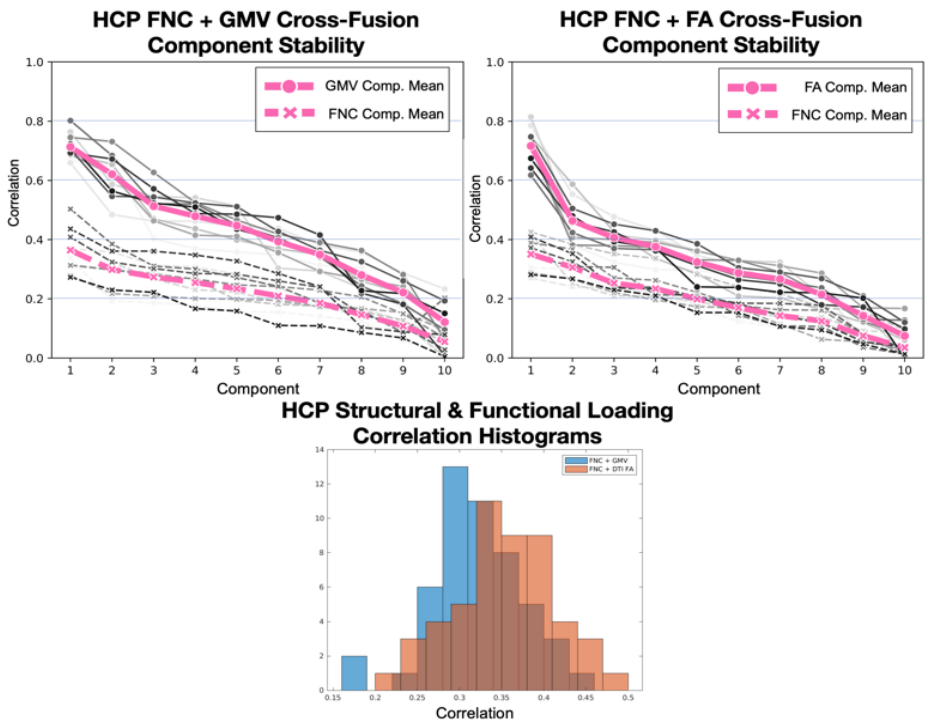

Fig.8. White matter (FA) components show one highly stable component, with a steep drop-off to dynamic components that show overall lower cross-fusion stability than corresponding GMV components in the same subjects (top row). Higher correlation between structural and functional loading parameters was observed in FA fusion experiments compared to GMV fusion (bottom row; $p = 0.0043$, $t = -2.927$).

Discussion

Here, we propose an approach for identifying flexible, dynamic linkages between brain structure and time-varying brain function, termed dynamic fusion. Though previous studies have examined time-resolved coupling of brain structure and function (Duda et al., 2022; Iraji et al., 2019; Liu et al., 2022; Plis et al., 2018), to the best of our knowledge our work is the first to jointly estimate voxel-wise structural components as a function of time, and thus as a function of structure's changing linkage to dynamic brain function. Our approach is fully data driven and allows both modalities (or all when 3+ modalities are used) to contribute to the fusion equally (i.e., symmetric fusion), thus enforcing fewer assumptions and

enabling a broader spectrum of flexibility than recent symmetric and asymmetric fusion works in structural dynamics. The findings outlined in this paper emphasize how conducting multiple linked fusions can greatly increase the versatility and interpretability of multimodal analyses.

We show that dynamic fusion identifies functionally adaptive neuroanatomical basis sets related to changing functional manifolds at both the window-level and dFNC state-level. To fully appreciate these results, we wish to underscore that the structural inputs are identical at each independent fusion within a given experiment, thus *any change in the resultant structural component maps is driven solely by its varying linkage to the changing functional inputs* at each window/state. In the HCP working memory task, we find the window-to-window cross-fusion stability of sMRI components directly aligns with known task boundaries (Fig. 2), further indicating that the functionally influenced changes to the neuroanatomical components captures changes in structure-function linkages that are indeed cognitively relevant. When applied in resting state data, we find only a few GMV components are consistently derived with high correspondence when jointly estimated with changing functional manifolds (Fig. 3), while the vast majority show evidence of more significant functional influences. These results held across numerous experiments encompassing different data sets (HCP vs. FBIRN), subject cohorts (CON vs. SZ), functional parcellations (data driven vs. atlas based), dynamic FNC approaches (SWPC vs. FBC), and even structural inputs (GMV vs. FA maps). Taken together, these results exemplify mCCA + jICA's capacity to identify truly joint linkages in the data to produce structural components that are indeed functionally influenced. Moreover, our findings underscore the importance of enabling flexible linkages between structure and function, especially as a function of the dynamic brain changes over time. Without the natural flexibility afforded by the mCCA + jICA algorithm, as well as the flexibility imparted by conducting multiple linked fusions as the novelty of the approach taken in this work, the nuanced joint structure-function relationships would have remained hidden in the data (Sui et al., 2013).

In addition to the cross-fusion stability of components aligning to changing cognitive demands across task/rest blocks in the working memory experiments, we found that a large portion (15/35) of dynamic components showed significant group differences between SZ and controls in the FBIRN resting state experiments, with a subset of dynamic GMV components exhibiting group differences on par with those of static components (Fig. 6). Based on this result, we can conclude functionally influenced structural components can indeed capture the changes in the relationship between structure and dynamic brain function of clinical and diagnostic relevance. By assessing the full structural/functional loading parameter space we also conclude that dynamic components show stronger separability along both structural and functional loading parameter axes than comparable static components, suggesting dynamic components do, indeed, represent a more harmonious joint influence of structure and function on the joint

source overall and thus better capture the complex interplay of structure and function underpinning both clinical and control populations.

Moreover, by applying dynamic fusion in a set of healthy control data from the HCP cohort we generated a map of global differential stability, organizing the brain into regions of static and dynamic functional linkages. We found static hubs aligned to the extremes of the unimodal (i.e., visual cortex) – transmodal (i.e., association cortex/anterior cingulate regions) hierarchy of cortical structures, whereas dynamic hubs were comprised of intermediary regions along this gradient (i.e., insular cortex) (Margulies et al., 2016). The significance of this result is two-fold: 1) it upholds and closely mirrors results of a recently published study which utilized multilinear regression to evaluate time-resolved structure-function coupling in atlas-derived brain networks (Liu et al., 2022), and 2) further underscores the neurobiological relevance of sources derived via our dynamic fusion approach.

It is thought that the unimodal-transmodal gradient reflects a similar gradient in connection lengths across the cortex (Oligschläger et al., 2019; Sepulcre et al., 2010). Thus, it is possible that the stability observed at the poles of this gradient are also a reflection of connection lengths – speculatively, this could stem from the ease of maintaining shorter connections and the importance of stabilizing critical long-range connections. In their work, (Liu et al., 2022) found this same U-shaped relationship between stability and connection length, with highest stability at the shortest and longest extremes and increased dynamicity for those networks with mid-range connection length. Our results corroborate this finding and warrant future exploration into connection lengths as a facet of structure-function dynamics.

One of the clearest dynamically linked structure-function hubs in both our study and (Liu et al., 2022) is the insula. The insula is a key region in the ventral attention/salience network that dynamically fields and coordinates communication of both unimodal (e.g., sensory) and transmodal (e.g., frontal) regions (Ghaziri et al., 2017; Tian & Zalesky, 2018). Taken together with our results, we echo the speculations presented in (Liu et al., 2022) and suggest that dynamic structure-function coupling exhibited within the insular cortex could reflect flexible integration and transmission of various neural signals though this complex cortical hub. Thus, states that result in dynamic structural components with peaks in insula could be thought of as "salience" states in which attention is being directed or integrated within the cortex.

This work represents a reduced-case feasibility study of a wider dynamic fusion framework (Fig 1). Our results clearly demonstrate the utility of estimating flexible linkages between structure and dynamic brain function, and thus motivate the extension of dynamic fusion to a more advanced model. In our next step, we plan to extend this work into a unified fusion framework that will jointly estimate multiple structural basis sets at once based on unique linkages between structural and temporally evolving functional inputs. In addition to the flexibility of coupling between neuroanatomical measures and

dynamic connections between functional networks, we may also consider incorporating flexibility in the structural definitions of the functional networks themselves. Future work could employ dynamic spatially constrained ICA (Duda et al., 2023; Iraji et al., 2019) to extract individualized time-varying functional entities with flexible spatial maps at each window in the dynamic analysis. Such an analysis could be done using the original 53 ICNs defines in the Neuromark_1.0 template, or be expanded to the multiscale Neuromark template (http://trendscenter.org/data), which defines 105 ICNs derived across multiple spatial and temporal scales (Iraji et al., 2023), further increasing the precision with which we can investigate dynamic structural and functional coupling in a data-driven manner.

Other future directions may involve extending the analyses described here by applying 3-way dynamic fusion to enable deeper investigation into the connection of both gray matter and white matter structure to temporally evolving brain function, as well as how hidden linkages between the structural modalities affect the joint estimation of the structural components. Interestingly, one result in our study suggested that white matter FA components were potentially more susceptible to functional influence in the joint fusion than GMV components in the same subjects (Fig. 8). Future work will be needed to replicate these results and further investigate the nature of white matter structure/gray matter function linkages. A newly developed ICA-based approach has enabled joint estimation of linked structural and functional connectivity from dMRI and fMRI data (Wu et al., 2015; Wu & Calhoun, 2023). Future work could leverage this approach under the dynamic fusion framework further address time varying structure-function linkages between white matter and FNC. Thus far, the analysis of brain function is largely focused on grey matter regions, leaving functional activity and connectivity within white matter regions relatively understudied. In fact, in data-driven analyses, functional components whose structural maps reside largely within white matter are often discarded as noise components. Exploration of the role of these white matter functional components in the context of whole brain function and cognition is currently underway. Future work including white matter functional components would further contextualize the investigation into dynamic structure-function coupling with tissue-level specificity on both ends.

In conclusion, we present an approach for dynamic fusion of multimodal neuroimaging data as a method for studying time-varying structure-function coupling. Components derived from our dynamic fusion approach exhibit strong cognitive, clinical and neurobiological correlates, underscoring the importance of retaining rich temporal dynamic information in studies of structure-function linkage. Overall, our results support the claim that patterns of structure-function coupling are both regionally heterogenous and temporally varying and provide an important next step in developing a model of dynamical linkage between brain function and structure.

References

Abrol, A., Rashid, B., Rachakonda, S., Damaraju, E., & Calhoun, V. D. (2017). Schizophrenia Shows Disrupted Links between Brain Volume and Dynamic Functional Connectivity. *Frontiers in Neuroscience*, *11*. https://www.frontiersin.org/articles/10.3389/fnins.2017.00624

Allen, E. A., Damaraju, E., Plis, S. M., Erhardt, E. B., Eichele, T., & Calhoun, V. D. (2014). Tracking whole-brain connectivity dynamics in the resting state. *Cerebral Cortex (New York, N.Y.: 1991)*, *24*(3), 663–676. https://doi.org/10.1093/cercor/bhs352

Andersson, J. L. R., Skare, S., & Ashburner, J. (2003). How to correct susceptibility distortions in spin-echo echo-planar images: Application to diffusion tensor imaging. *NeuroImage*, *20*(2), 870–888. https://doi.org/10.1016/S1053-8119(03)00336-7

Andersson, J. L. R., & Sotiropoulos, S. N. (2016). An integrated approach to correction for off-resonance effects and subject movement in diffusion MR imaging. *NeuroImage*, *125*, 1063–1078. https://doi.org/10.1016/j.neuroimage.2015.10.019

Avants, B. B., Tustison, N., & Johnson, H. (2009). Advanced Normalization Tools (ANTS). *Insight J*, *2*(365), 1–35.

Battaglia, D., Boudou, T., Hansen, E. C. A., Lombardo, D., Chettouf, S., Daffertshofer, A., McIntosh, A. R., Zimmermann, J., Ritter, P., & Jirsa, V. (2020). Dynamic Functional Connectivity between order and randomness and its evolution across the human adult lifespan. *NeuroImage*, *222*, 117156. https://doi.org/10.1016/j.neuroimage.2020.117156

Baum, G. L., Cui, Z., Roalf, D. R., Ciric, R., Betzel, R. F., Larsen, B., Cieslak, M., Cook, P. A., Xia, C. H., Moore, T. M., Ruparel, K., Oathes, D. J., Alexander-Bloch, A. F., Shinohara, R. T., Raznahan, A., Gur, R. E., Gur, R. C., Bassett, D. S., & Satterthwaite, T. D. (2020). Development of structure–function coupling in human brain networks during youth. *Proceedings of the National Academy of Sciences*, *117*(1), 771–778. https://doi.org/10.1073/pnas.1912034117

Calhoun, V. D., Miller, R., Pearlson, G., & Adalı, T. (2014). The Chronnectome: Time-Varying Connectivity Networks as the Next Frontier in fMRI Data Discovery. *Neuron*, *84*(2), 262–274. https://doi.org/10.1016/j.neuron.2014.10.015

Calhoun, V. D., & Sui, J. (2016). Multimodal Fusion of Brain Imaging Data: A Key to Finding the Missing Link(s) in Complex Mental Illness. *Biological Psychiatry: Cognitive Neuroscience and Neuroimaging*, *1*(3), 230–244. https://doi.org/10.1016/j.bpsc.2015.12.005

Calhoun, V., Wu, L., Kiehl, K., Eichele, T., & Pearlson, G. (2010). Aberrant Processing of Deviant Stimuli in Schizophrenia Revealed by Fusion of FMRI and EEG Data. *Acta Neuropsychiatrica*, *22*(3), 127–138. https://doi.org/10.1111/j.1601-5215.2010.00467.x

Chang, C., & Glover, G. H. (2010). Time–frequency dynamics of resting-state brain connectivity measured with fMRI. *NeuroImage*, *50*(1), 81–98. https://doi.org/10.1016/j.neuroimage.2009.12.011

Damaraju, E., Allen, E. A., Belger, A., Ford, J. M., McEwen, S., Mathalon, D. H., Mueller, B. A., Pearlson, G. D., Potkin, S. G., Preda, A., Turner, J. A., Vaidya, J. G., van Erp, T. G., & Calhoun, V. D. (2014). Dynamic functional connectivity analysis reveals transient states of dysconnectivity in schizophrenia. *NeuroImage. Clinical*, *5*, 298–308. https://doi.org/10.1016/j.nicl.2014.07.003

DeRamus, T. P., Wu, L., Qi, S., Iraji, A., Silva, R., Du, Y., Pearlson, G., Mayer, A., Bustillo, J. R., Stromberg, S. F., & Calhoun, V. D. (2022). Multimodal data fusion of cortical-subcortical morphology and functional network connectivity in psychotic spectrum disorder. *NeuroImage. Clinical*, *35*, 103056. https://doi.org/10.1016/j.nicl.2022.103056

Du, Y., Fu, Z., Sui, J., Gao, S., Xing, Y., Lin, D., Salman, M., Abrol, A., Rahaman, M. A., Chen, J., Hong, L. E., Kochunov, P., Osuch, E. A., Calhoun, V. D., & Alzheimer's Disease Neuroimaging Initiative. (2020). NeuroMark: An automated and adaptive ICA based pipeline to identify reproducible fMRI markers of brain disorders. *NeuroImage. Clinical*, *28*, 102375. https://doi.org/10.1016/j.nicl.2020.102375

Duda, M., Faghiri, A., & Calhoun, V. D. (2022). Multimodal Analysis Uncovers Links between Grey Matter Volume and both Low-and High-frequency Dynamic Connectivity States in Schizophrenia. *2022 IEEE International Conference on Bioinformatics and Biomedicine (BIBM)*, 1521–1525. https://doi.org/10.1109/BIBM55620.2022.9995415

Duda, M., Iraji, A., Ford, J. M., Lim, K. O., Mathalon, D. H., Mueller, B. A., Potkin, S. G., Preda, A., Van Erp, T. G. M., & Calhoun, V. D. (2023). Reliability and clinical utility of spatially constrained estimates of intrinsic functional networks from very short fMRI scans. *Human Brain Mapping*, *44*(6), 2620–2635. https://doi.org/10.1002/hbm.26234

Faghiri, A., Iraji, A., Damaraju, E., Turner, J., & Calhoun, V. D. (2021). A unified approach for characterizing static/dynamic connectivity frequency profiles using filter banks. *Network Neuroscience*, *5*(1), 56–82. https://doi.org/10.1162/netn_a_00155

Fukushima, M., Betzel, R. F., He, Y., van den Heuvel, M. P., Zuo, X.-N., & Sporns, O. (2018). Structure-function relationships during segregated and integrated network states of human brain functional connectivity. *Brain Structure & Function*, *223*(3), 1091–1106. https://doi.org/10.1007/s00429-017-1539-3

Fukushima, M., & Sporns, O. (2020). Structural determinants of dynamic fluctuations between segregation and integration on the human connectome. *Communications Biology*, *3*(1), Article 1. https://doi.org/10.1038/s42003-020-01331-3

Geenjaar, E. P. T., Lewis, N. L., Fedorov, A., Wu, L., Ford, J. M., Preda, A., Plis, S. M., & Calhoun, V. D. (2023). Chromatic fusion: Generative multimodal neuroimaging data fusion provides multi-informed insights into schizophrenia. *medRxiv*, 2023.05.18.23290184. https://doi.org/10.1101/2023.05.18.23290184

Ghaziri, J., Tucholka, A., Girard, G., Houde, J.-C., Boucher, O., Gilbert, G., Descoteaux, M., Lippé, S., Rainville, P., & Nguyen, D. K. (2017). The Corticocortical Structural Connectivity of the Human Insula. *Cerebral Cortex*, *27*(2), 1216–1228. https://doi.org/10.1093/cercor/bhv308

Glasser, M. F., Coalson, T. S., Robinson, E. C., Hacker, C. D., Harwell, J., Yacoub, E., Ugurbil, K., Andersson, J., Beckmann, C. F., Jenkinson, M., Smith, S. M., & Van Essen, D. C. (2016). A multi-modal parcellation of human cerebral cortex. *Nature*, *536*(7615), Article 7615. https://doi.org/10.1038/nature18933

Griffa, A., Amico, E., Liégeois, R., Van De Ville, D., & Preti, M. G. (2022). Brain structure-function coupling provides signatures for task decoding and individual fingerprinting. *NeuroImage*, *250*, 118970. https://doi.org/10.1016/j.neuroimage.2022.118970

Iraji, A., Deramus, T. P., Lewis, N., Yaesoubi, M., Stephen, J. M., Erhardt, E., Belger, A., Ford, J. M., McEwen, S., Mathalon, D. H., Mueller, B. A., Pearlson, G. D., Potkin, S. G., Preda, A., Turner, J. A., Vaidya, J. G., van Erp, T. G. M., & Calhoun, V. D. (2019). The spatial chronnectome reveals a dynamic interplay between functional segregation and integration. *Human Brain Mapping*, *40*(10), 3058–3077. https://doi.org/10.1002/hbm.24580

Iraji, A., Faghiri, A., Lewis, N., Fu, Z., Rachakonda, S., & Calhoun, V. D. (2021). Tools of the trade: Estimating time-varying connectivity patterns from fMRI data. *Social Cognitive and Affective Neuroscience*, *16*(8), 849–874. https://doi.org/10.1093/scan/nsaa114

Iraji, A., Fu, Z., Faghiri, A., Duda, M., Chen, J., Rachakonda, S., DeRamus, T., Kochunov, P., Adhikari, B. M., Belger, A., Ford, J. M., Mathalon, D. H., Pearlson, G. D., Potkin, S. G., Preda, A., Turner, J. A., van Erp, T. G. M., Bustillo, J. R., Yang, K., … Calhoun, V. D. (2023). Identifying canonical and replicable multi-scale intrinsic connectivity networks in 100k+ resting-state fMRI datasets. *Human Brain Mapping*, *44*(17), 5729–5748. https://doi.org/10.1002/hbm.26472

Keator, D. B., van Erp, T. G. M., Turner, J. A., Glover, G. H., Mueller, B. A., Liu, T. T., Voyvodic, J. T., Rasmussen, J., Calhoun, V. D., Lee, H. J., Toga, A. W., McEwen, S., Ford, J. M., Mathalon, D. H., Diaz, M., O'Leary, D. S., Jeremy Bockholt, H., Gadde, S., Preda, A., … FBIRN. (2016). The Function Biomedical Informatics Research Network Data Repository. *NeuroImage*, *124*(Pt B), 1074–1079. https://doi.org/10.1016/j.neuroimage.2015.09.003

Khalilullah, K. M. I., Agcaoglu, O., Sui, J., Adali, T., Duda, M., & Calhoun, V. D. (2023). Multimodal fusion of multiple rest fMRI networks and MRI gray matter via multilink joint ICA reveals highly significant function/structure coupling in Alzheimer's disease. *bioRxiv: The Preprint Server for Biology*, 2023.02.28.530458. https://doi.org/10.1101/2023.02.28.530458

Liu, Z.-Q., Vázquez-Rodríguez, B., Spreng, R. N., Bernhardt, B. C., Betzel, R. F., & Misic, B. (2022). Time-resolved structure-function coupling in brain networks. *Communications Biology*, *5*(1), Article 1. https://doi.org/10.1038/s42003-022-03466-x

Lottman, K. K., White, D. M., Kraguljac, N. V., Reid, M. A., Calhoun, V. D., Catao, F., & Lahti, A. C. (2018). Four-way multimodal fusion of 7 T imaging data using an mCCA+jICA model in first-episode schizophrenia. *Human Brain Mapping*, *39*(4), 1475–1488. https://doi.org/10.1002/hbm.23906

Lurie, D. J., Kessler, D., Bassett, D. S., Betzel, R. F., Breakspear, M., Kheilholz, S., Kucyi, A., Liégeois, R., Lindquist, M. A., McIntosh, A. R., Poldrack, R. A., Shine, J. M., Thompson, W. H., Bielczyk, N. Z., Douw, L., Kraft, D., Miller, R. L., Muthuraman, M., Pasquini, L., … Calhoun, V. D. (2020). Questions and controversies in the study of time-varying functional connectivity in resting fMRI. *Network Neuroscience*, *4*(1), 30–69. https://doi.org/10.1162/netn_a_00116

Margulies, D. S., Ghosh, S. S., Goulas, A., Falkiewicz, M., Huntenburg, J. M., Langs, G., Bezgin, G., Eickhoff, S. B., Castellanos, F. X., Petrides, M., Jefferies, E., & Smallwood, J. (2016). Situating the default-mode network along a principal gradient of macroscale cortical organization. *Proceedings of the National Academy of Sciences*, *113*(44), 12574–12579. https://doi.org/10.1073/pnas.1608282113

Oligschläger, S., Xu, T., Baczkowski, B. M., Falkiewicz, M., Falchier, A., Linn, G., & Margulies, D. S. (2019). Gradients of connectivity distance in the cerebral cortex of the macaque monkey. *Brain Structure and Function*, *224*(2), 925–935. https://doi.org/10.1007/s00429-018-1811-1

Pang, J. C., Aquino, K. M., Oldehinkel, M., Robinson, P. A., Fulcher, B. D., Breakspear, M., & Fornito, A. (2023). Geometric constraints on human brain function. *Nature*, *618*(7965), Article 7965. https://doi.org/10.1038/s41586-023-06098-1

Plis, S. M., Amin, M. F., Chekroud, A., Hjelm, D., Damaraju, E., Lee, H. J., Bustillo, J. R., Cho, K., Pearlson, G. D., & Calhoun, V. D. (2018). Reading the (functional) writing on the (structural) wall: Multimodal fusion of brain structure and function via a deep neural network based translation approach reveals novel impairments in schizophrenia. *NeuroImage*, *181*, 734–747. https://doi.org/10.1016/j.neuroimage.2018.07.047

Preti, M. G., Bolton, T. A., & Van De Ville, D. (2017). The dynamic functional connectome: State-of-the-art and perspectives. *NeuroImage*, *160*, 41–54. https://doi.org/10.1016/j.neuroimage.2016.12.061

Preti, M. G., & Van De Ville, D. (2019). Decoupling of brain function from structure reveals regional behavioral specialization in humans. *Nature Communications*, *10*(1), Article 1. https://doi.org/10.1038/s41467-019-12765-7

Qi, S., Silva, R. F., Zhang, D., Plis, S. M., Miller, R., Vergara, V. M., Jiang, R., Zhi, D., Sui, J., & Calhoun, V. D. (2022). Three-way parallel group independent component analysis: Fusion of spatial and spatiotemporal magnetic resonance imaging data. *Human Brain Mapping*, *43*(4), 1280–1294. https://doi.org/10.1002/hbm.25720

Sepulcre, J., Liu, H., Talukdar, T., Martincorena, I., Yeo, B. T. T., & Buckner, R. L. (2010). The Organization of Local and Distant Functional Connectivity in the Human Brain. *PLOS Computational Biology*, *6*(6), e1000808. https://doi.org/10.1371/journal.pcbi.1000808

Sui, J., Adali, T., Yu, Q., Chen, J., & Calhoun, V. D. (2012). A review of multivariate methods for multimodal fusion of brain imaging data. *Journal of Neuroscience Methods*, *204*(1), 68–81. https://doi.org/10.1016/j.jneumeth.2011.10.031

Sui, J., He, H., Pearlson, G. D., Adali, T., Kiehl, K. A., Yu, Q., Clark, V. P., Castro, E., White, T., Mueller, B. A., Ho, B. C., Andreasen, N. C., & Calhoun, V. D. (2013). Three-way (N-way) fusion of brain

imaging data based on mCCA+jICA and its application to discriminating schizophrenia. *NeuroImage*, *66*, 119–132. https://doi.org/10.1016/j.neuroimage.2012.10.051

Sui, J., Pearlson, G., Caprihan, A., Adali, T., Kiehl, K. A., Liu, J., Yamamoto, J., & Calhoun, V. D. (2011). Discriminating schizophrenia and bipolar disorder by fusing fMRI and DTI in a multimodal CCA+ joint ICA model. *NeuroImage*, *57*(3), 839–855. https://doi.org/10.1016/j.neuroimage.2011.05.055

Tian, Y., & Zalesky, A. (2018). Characterizing the functional connectivity diversity of the insula cortex: Subregions, diversity curves and behavior. *NeuroImage*, *183*, 716–733. https://doi.org/10.1016/j.neuroimage.2018.08.055

Van Essen, D. C., Smith, S. M., Barch, D. M., Behrens, T. E. J., Yacoub, E., & Ugurbil, K. (2013). The WU-Minn Human Connectome Project: An overview. *NeuroImage*, *80*, 62–79. https://doi.org/10.1016/j.neuroimage.2013.05.041

Vázquez-Rodríguez, B., Suárez, L. E., Markello, R. D., Shafiei, G., Paquola, C., Hagmann, P., van den Heuvel, M. P., Bernhardt, B. C., Spreng, R. N., & Misic, B. (2019). Gradients of structure-function tethering across neocortex. *Proceedings of the National Academy of Sciences of the United States of America*, *116*(42), 21219–21227. https://doi.org/10.1073/pnas.1903403116

Wu, L., & Calhoun, V. (2023). Joint connectivity matrix independent component analysis: Auto-linking of structural and functional connectivities. *Human Brain Mapping*, *44*(4), 1533–1547. https://doi.org/10.1002/hbm.26155

Wu, L., Calhoun, V. D., Jung, R. E., & Caprihan, A. (2015). Connectivity-based whole brain dual parcellation by group ICA reveals tract structures and decreased connectivity in schizophrenia. *Human Brain Mapping*, *36*(11), 4681–4701. https://doi.org/10.1002/hbm.22945